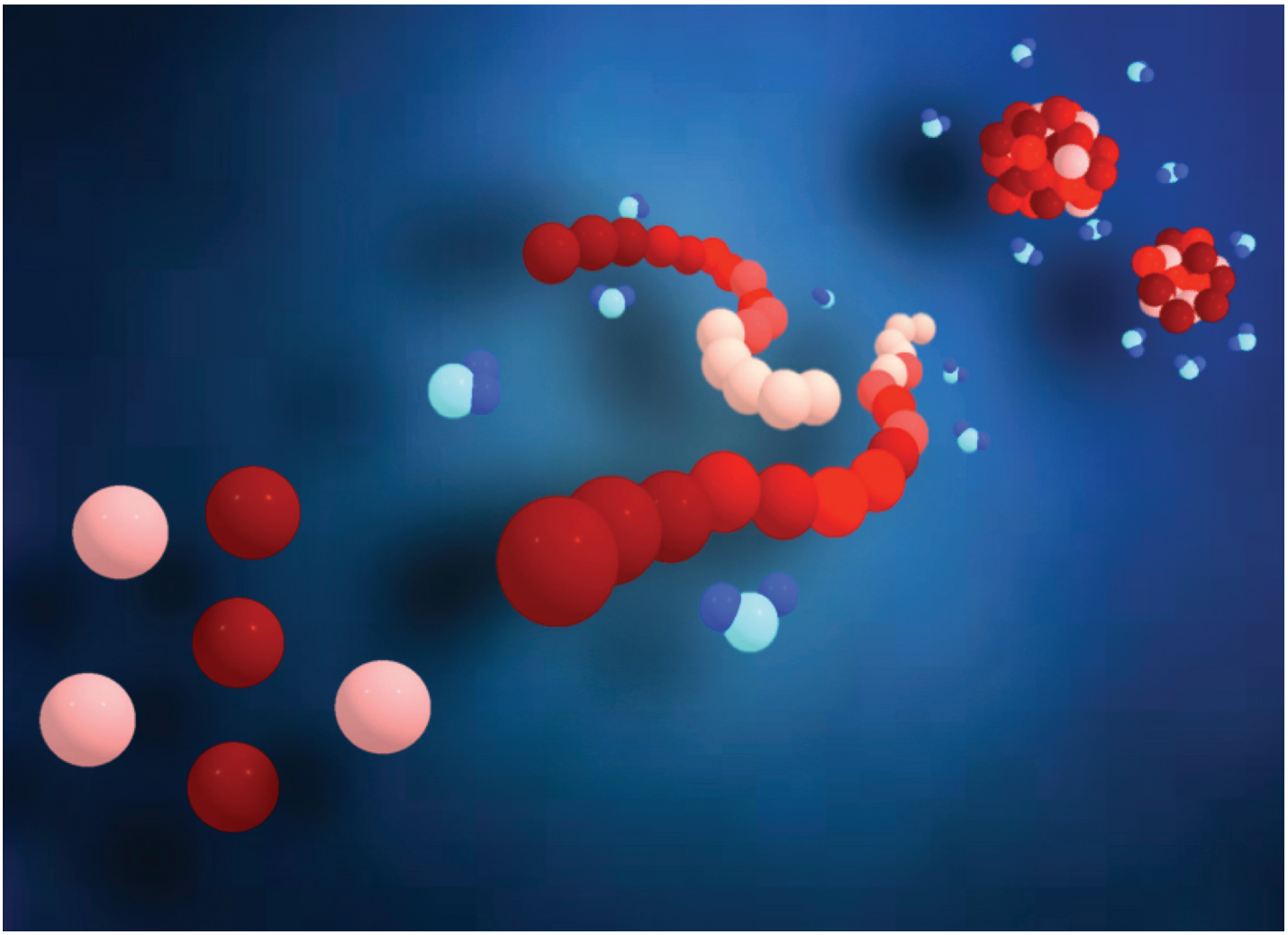

Highlighting research results from the Université Paul Sabatier Toulouse III, France, Friedrich-Schiller University, Germany and CIQA, Mexico.

Thermosensitive spontaneous gradient copolymers with block- and gradient-like features

Simon Harrisson, Carlos Guerrero Sanchez and coworkers use RAFT copolymerization combined with high-throughput experimentation to prepare spontaneous gradient copolymers of *N*-isopropyl acrylamide (NIPAM) and vinyl acetate (VAc). These copolymers have thermoresponsive and self-assembly characteristics resembling those of NIPAM-VAc block copolymers but with some intriguing differences. Their synthetic approach could readily be adapted to other comonomer systems to provide an accessible and economic alternative to the conventional multi-step preparation of block copolymers.

As featured in:

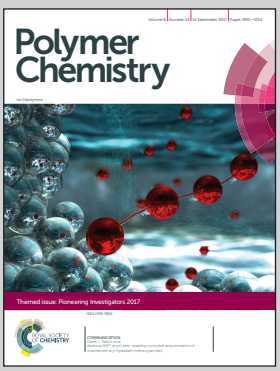

See Carlos Guerrero-Sanchez, Simon Harrisson *et al.*, *Polym. Chem.*, 2017, **8**, 5023.

ROYAL SOCIETY OF CHEMISTRY

rsc.li/polymers

Registered charity number: 207890

Polymer Chemistry

PAPER

View Article Online
View Journal | View Issue

Cite this: *Polym. Chem.*, 2017, **8**, 5023

Thermosensitive spontaneous gradient copolymers with block- and gradient-like features†

Roberto Yañez-Macias,[a,b] Ihor Kulai,[c] Jens Ulbrich,[b] Turgay Yildirim,[b,d] Pelin Sungur,[b,d] Stephanie Hoeppener,[b,d] Ramiro Guerrero-Santos,[a] Ulrich S. Schubert,[b,d] Mathias Destarac,[c] Carlos Guerrero-Sanchez*[b,d] and Simon Harrisson*[c]

Received 23rd March 2017,
Accepted 19th April 2017

DOI: 10.1039/c7py00495h

rsc.li/polymers

Reversible addition–fragmentation chain transfer (RAFT) copolymerization was used to prepare copolymers of *N*-isopropyl acrylamide (NIPAM) and vinyl acetate (VAc) with mole fractions of NIPAM ranging from 0.1 to 0.6 and targeted degrees of polymerization of 100 and 250. The measured kinetic parameters and obtained experimental results revealed that this copolymerization system leads to a "one pot" synthesis of amphiphilic gradient copolymers, which have thermoresponsive and self-assembly characteristics resembling those of the analogous block copolymers but with some intriguing differences. Their self-assembly behavior in water suggests the formation of dynamic aggregates which respond rapidly to changes in solubility as revealed by ^{1}H NMR spectroscopy, in contrast to the kinetically frozen aggregates formed by block copolymers. Furthermore, despite their block-like composition profiles, these copolymers display a single and broad glass transition, as is typically found in linear gradient copolymers. The synthetic approach presented in this contribution could readily be adapted to other comonomer systems to provide an accessible and economic alternative to the conventional multi-step preparation of block copolymers.

Introduction

Thermoresponsive polymers exhibit a step change in properties in response to a change in temperature.[1] A typical example is poly(*N*-isopropyl acrylamide) (PNIPAM), which is soluble in water below its lower critical solution temperature (LCST) of around 32 °C and precipitates above this temperature.[2] Block copolymers that incorporate one or more thermoresponsive blocks show self-assembly behavior that is sensitive to changes in temperature.[3] This behavior is of interest for applications including drug-delivery[4] and stimuli-responsive gel formation.[5,6]

Block copolymers are typically prepared by sequential monomer addition: the synthesis of the first block is followed by its use as an initiator or chain transfer agent in the preparation of the second block.[7] These reactions, and their associated purification steps, can be time-consuming, while the accumulation of small variations in each step may lead to lower reproducibility, an important criterion for biomedical applications.

Spontaneous gradient copolymers[8] represent an attractive alternative to block copolymers. Prepared by direct reversible deactivation radical copolymerization of two monomers of different reactivity in a batch process, they combine simplicity of access with a degree of architectural control.[9–13] Moreover, if at least one of the monomers has a strong tendency to alternate (reactivity ratio $\lesssim$0.2), spontaneous gradient copolymers with block-like architectures may be prepared.[11–13]

In this study, we report the reversible addition–fragmentation chain transfer (RAFT) copolymerization of *N*-isopropyl acrylamide (NIPAM) and vinyl acetate (VAc) to form thermoresponsive spontaneous gradient copolymers. VAc is poorly incorporated in copolymerization with NIPAM[14] and so is a good candidate for the formation of spontaneous gradient copolymers. In addition, poly(vinyl acetate) (PVAc) is an attractive hydrophobic component due to its wide range of appli-

[a]*Centro de Investigación en Química Aplicada, Departamento de Síntesis de Polímeros, (CIQA), Boulevard Enrique Reyna No. 140, 25294 Saltillo, Mexico*
[b]*Laboratory of Organic and Macromolecular Chemistry (IOMC), Friedrich Schiller University Jena, Humboldtstr. 10, D-07743 Jena, Germany.*
E-mail: carlos.guerrero.sanchez@uni-jena.de
[c]*Laboratoire des IMRCP, Université de Toulouse, CNRS UMR 5623, Université Paul Sabatier, 118 route de Narbonne, 31062 Toulouse Cedex 9, France.*
E-mail: polyharrisson@gmail.com
[d]*Jena Center for Soft Matter (JCSM), Friedrich Schiller University Jena, Philosophenweg 7, D-07743 Jena, Germany*

†Electronic supplementary information (ESI) available. See DOI: 10.1039/c7py00495h

cations as a binder for wound dressings, as an adhesive, and as a precursor to poly(vinyl alcohol).[15,16]

A xanthate-based RAFT agent was chosen as these compounds are highly effective in controlling the polymerization of vinyl esters,[17] while also providing reasonable control over the polymerization of acrylamides[18] and acrylates.[19,20] This allows block[18,21,22] and gradient[11] copolymers of these monomers to be prepared without resorting to the use of switchable RAFT agents[23] or orthogonal polymerization strategies.[24]

In addition, a major part of this investigation was performed in a commercially available automated parallel synthesizer.[11,20,25–27] The use of this well-established high-throughput experimental technique[11,25–27] enabled us to rapidly perform a detailed kinetic investigation of this reaction system. The methodical variation of different reaction parameters over a broad range (*e.g.*, comonomer composition, reagent concentration, reaction time, *etc*.) allowed us to obtain a copolymer library with a systematic variation in copolymer composition and molar mass, and experimental kinetic data for the estimation of the reactivity ratios of this copolymerization system.

Experimental

Materials

VAc (>99%, TCI) was purified by stirring in presence of inhibitor-remover for hydroquinone (Aldrich) for 30 minutes prior to use. *O*-ethyl-*S*-(1-methoxycarbonyl)ethyl xanthate was synthesized according to a literature procedure.[28] NIPAM (≥99%, Aldrich), 2,2′-azobis-(isobutyronitrile) (AIBN, Aldrich), methanol, 1,4-dioxane and 1,3,5-trioxane (≥99%, Aldrich) were used as received.

Gradient copolymer synthesis

Copolymerizations were performed in a Chemspeed Accelerator SLT automated parallel synthesizer using a sequential reagent addition and similar experimental protocols as reported elsewhere.[11,25–27] In a typical experiment: VAc and stock solutions of NIPAM (337 mg mL^{-1} in dioxane/methanol 1 : 1 mixture), *O*-ethyl-*S*-(1-methoxycarbonyl)ethyl xanthate (73 mg mL^{-1} in dioxane/methanol 1 : 1 mixture) and AIBN (7.2 mg mL^{-1} in dioxane/methanol 1 : 1 mixture) were prepared, degassed by sparging with inert gas for 15 min in an ice bath and placed inside the automated synthesizer. Afterwards, for each investigated series, aliquots of VAc, prepared stock solutions and solvent were transferred from the containers into different reactors (13 mL) of the synthesizer with the automated liquid handling system to provide the desired concentration of reagents resulting in a final volume of 5.23 mL (note that volume changes due to mixing of the reagents have been neglected). 1,3,5-Trioxane dissolved in the NIPAM solution was used as internal standard at a concentration of 10 mg mL^{-1} of total reaction volume. Once in the reactor, the reaction mixture was subjected to a degassing procedure in the parallel synthesizer as described elsewhere.[11,25–27] Thereafter, the reaction mixtures were heated to 70 °C for 15 h. Table 1 summarizes the amounts and ratios used in each reactor. The obtained samples were labeled with a capital letter followed by a numeric sub-index representing initial monomer feed ratios of NIPAM and VAc, respectively. For example, label $\mathbf{A}_{20/80}$ corresponds to sample with a target DP = 250 containing 20% mol of NIPAM and 80% mol of VAc. Additional polymerizations were carried out at 20 mol% and 50 mol% NIPAM in order to refine the estimated reactivity ratios. Details of these polymerizations are given in the ESI.†

Table 1 Overview of the selected reaction conditions used for the copolymerizations of VAc and NIPAM using an automated parallel synthesizer

Entry	[M/RAFT][a]	$f_{NIPAM,\ ini}$	$f_{VAc,\ ini}$	$n_{NIPAM,\ ini}$ (mmol)	$n_{VAc,\ ini}$ (mmol)
$A_{10/90}$	250	0.1	0.9	2.0	18
$A_{20/80}$	250	0.2	0.8	4.0	16
$A_{30/70}$	250	0.3	0.7	6.0	14
$A_{40/60}$	250	0.4	0.6	8.0	12
$A_{50/50}$	250	0.5	0.5	10	10
$A_{60/40}$	250	0.6	0.4	12	8.0
$B_{10/90}$	100	0.1	0.9	2.0	18
$B_{20/80}$	100	0.2	0.8	4.0	16
$B_{30/70}$	100	0.3	0.7	6.0	14
$B_{40/60}$	100	0.4	0.6	8.0	12
$B_{50/50}$	100	0.5	0.5	10	10
$B_{60/40}$	100	0.6	0.4	12	8.0

[a] [RAFT]/[AIBN] = 1/0.13.

Kinetic studies of the copolymerizations

During each polymerization, aliquots of 0.2 mL were taken periodically (0.5, 1, 1.5, 2, 6 and 15 h) under an inert gas flow. For each sample, conversions were calculated by proton nuclear magnetic resonance (^{1}H NMR) using 1,3,5-trioxane as internal standard in deuterated chloroform ($CDCl_3$). Molar masses and dispersities were determined *via* size exclusion chromatography (SEC) analysis.

Block copolymer synthesis

NIPAM (0.453 g, 0.679 g or 0.905 g for $\mathbf{A}'_{20/80}$, $\mathbf{A}'_{30/70}$ or $\mathbf{A}'_{40/60}$, respectively) and 3 mL of stock solution of *O*-ethyl-*S*-(1-methoxycarbonyl)ethyl xanthate and AIBN (5.56 mg mL^{-1} and 0.556 mg mL^{-1} respectively in dioxane/methanol 1 : 1 mixture) were mixed, degassed by sparging with inert gas for 30 min in a 16 mL reactor and placed in a heating block that was thermostated at 70 °C. After heating for 2.25 h, NIPAM conversions of 92–94% were reached.

Then, VAc (1.377 g, 1.290 g or 1.106 g for $\mathbf{A}'_{20/80}$, $\mathbf{A}'_{30/70}$ or $\mathbf{A}'_{40/60}$, respectively), degassed by sparging with inert gas for 30 min was added and heating was continued for 90 h sampling at programmed times. The polymers were isolated by drying under reduced pressure, redissolved in deionized water and freeze-dried.

Instruments and methods

^{1}H NMR spectra were recorded on a Bruker AC 300 (300 MHz) spectrometer at room temperature. The chemical shifts are reported in parts per million (ppm, δ scale) relative to the signals from the NMR solvents.

^{1}H NMR spectra with variation of temperature. Polymer solutions in D_2O were prepared at a concentration of 10 mg mL^{-1} by direct dissolution of the polymer sample at 4 °C over 24 h. The sample was heated in a tube from 25 to 35 °C in 2 °C steps. At each temperature step, the sample was equilibrated for 300 s and a ^{1}H NMR spectrum was recorded. 1,4-Dioxane (~50 ppm) was used as an internal standard for the signal integration.

SEC measurements were performed on a Shimadzu system equipped with a SCL-10A system controller, a LC-10AD pump, a RID-10A refractive index detector, and a PSSSDV-linear S column (5 μm particle size; Polymer Standards Service GmbH, Mainz, Germany) at 40 °C using a chloroform ($CHCl_3$), triethylamine and 2-propanol (94 : 4 : 2) mixture as eluent at a flow rate of 1 mL min^{-1}. The system was calibrated with a linear curve built from polystyrene standards (M_p = 370 to 128 000 g mol^{-1}).

Dynamic light scattering (DLS). Hydrodynamic diameters were determined using a Zetasizer Nano-ZS (Malvern Instruments, Ltd, UK) with integrated 4 mW He–Ne laser, λ = 633 nm. The correlation function was analyzed *via* the cumulant method to obtain the *Z*-average size and polydispersity of the colloids and by the general purpose method (NNLS) to obtain the distribution of diffusion coefficients of the solutes. The apparent equivalent hydrodynamic diameter was then determined using the Stokes–Einstein equation. The sample was heated in a cuvette from 25 to 35 °C in 2 °C steps. At each temperature step, the sample was equilibrated for 300 s and then measured in triplicate. Polymer solutions were prepared at a concentration of 10 mg mL^{-1} by direct dissolution of the polymer sample in ultrapure water at 4 °C over 24 h.

Differential scanning calorimetry (DSC). Thermal analyses were carried out on a Netzsch DSC 204 F1 Phoenix instrument under a nitrogen atmosphere. The prepared samples were first heated to 180 °C and kept at this temperature for 5 min to erase any prior thermal history. Then two cycles were recorded from −25 to 180 °C at cooling and heating rates of 20 K min^{-1}. The glass transition temperature (T_g) values are reported for the second heating run.

Cryogenic transmission electron microscopy (cryo-TEM). Measurements were performed on a FEI Tecnai G^2 20 operating at an acceleration voltage of 200 kV. Images were recorded with a side-entry MegaView (OSIS) camera.

For the temperature-dependent investigation, the samples were preheated under agitation for at least 30 min in a water bath at 35 °C. A drop of the polymer solution (8.5 μL) was rapidly placed with atmosphere Vibrobot Mark IV plunging stage. The temperature within the Vibrobot chamber was adjusted to 38 °C. The samples were rapidly blotted and plunged into a cryogen reservoir containing liquid ethane. The holder was cooled and samples were maintained at a temperature below −176 °C at all times.

Determination of reactivity ratios. Point estimates and joint confidence intervals for reactivity ratios were determined using the visualization of the sum of squares method developed by van den Brink *et al.*[29] The integrated copolymerization equation was fitted to conversion and monomer feed composition data, assuming non-negligible errors in all variables. Simulated copolymer sequences were calculated as Markov chains according to the method described in Harrisson *et al.*[12] The probabilities that a NIPAM unit is followed by another NIPAM unit or that a VAc unit is followed by another VAc unit are given by eqn (1) and (2).

$$P(\mathrm{NIPAM}|\mathrm{NIPAM})_n = \frac{r_{\mathrm{NIPAM}} f_{\mathrm{NIPAM},x}}{f_{\mathrm{VAc},x} + r_{\mathrm{NIPAM}} f_{\mathrm{NIPAM},x}} \quad (1)$$

$$P(\mathrm{VAc}|\mathrm{VAc})_n = \frac{r_{\mathrm{VAc}} f_{\mathrm{VAc},x}}{f_{\mathrm{NIPAM},x} + r_{\mathrm{VAc}} f_{\mathrm{VAc},x}} \quad (2)$$

where $P(i|j)_n$ is the probability that the unit in the n^{th} position, corresponding to the conversion x ($x = n/\mathrm{DP}_{\mathrm{target}}$) will be i if the preceding unit is j, $f_{i,x}$ is the mole fraction of i at conversion x, and r_i is the reactivity ratio of i. All analysis was performed using Microsoft Excel software.

Results and discussion

Synthesis and characterization of P(NIPAM-*grad*-VAc) gradient copolymers

The effectiveness of RAFT agents **1** (Scheme 1) is determined by the substituents R and Z.[30] The R group must be a good homolytic leaving group with respect to the propagating radical in order to promote fragmentation of the intermediate **2** to the desired products **3**. It must also be able to reinitiate the polymerization at a similar rate to that of propagation.[31] The Z group primarily affects the stability of the intermediate radical and the reactivity of the thiocarbonyl group towards radical addition.[32]

The ability of radically polymerizable monomers to react in a free radical process gives rise to two general groups; the "more activated monomers" (MAMs), and the "less activated monomers" (LAMs). MAMs, such as NIPAM, give propagating radicals that possess low reactivity in radical addition due to the enhanced electronic stabilization and steric factors.[7] Their polymerization is well controlled by active RAFT agents as dithioesters (Z = aryl or alkyl) and trithiocarbonates (Z = *S*-alkyl).

On the other hand, LAMs, such as VAc, generate more reactive macro-radicals, requiring less active transfer agents such

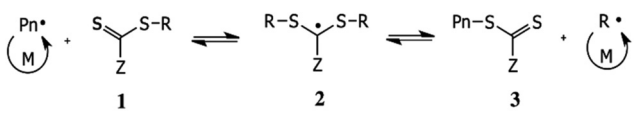

Scheme 1 Simplified RAFT mechanism.

as dithiocarbamates (Z = NR′$_2$)[33] and xanthates (Z = OR′).[17] Use of more active RAFT agents to control the polymerization of LAMs generally results in complete inhibition of polymerization, as poly(LAM) macroradicals are relatively poor leaving groups, which delays the fragmentation process.

By contrast, less active RAFT agents such as xanthates provide a moderate level of control over many MAM polymerizations, including those of acrylamides[34] and acrylates.[19] Thus, xanthate-based RAFT agents are a natural choice to control the copolymerization of VAc with more activated monomers.[11] For this study, *O*-ethyl-*S*-1-methoxycarbonylethyl xanthate was selected as a RAFT agent to carry out copolymerization of VAc with NIPAM in dioxane/methanol mixture at 70 °C using AIBN as source of radicals, as detailed in Scheme 2.

High-throughput synthesis techniques were used to investigate in detail the evolution of molar mass and conversion of the spontaneous gradient copolymers. The automated liquid handling system of a commercially available parallel synthesizer was used to perform normally time-consuming protocols such as transferring the liquids into each reactor, degassing,[27] and collecting samples for SEC and NMR analyses under inert conditions, in order to determine kinetic parameters accurately.

Monomer conversions were tracked by NMR spectroscopy (Fig. S1 in ESI†) and fitted to the terminal polymerization model using non-linear least squares fitting assuming errors in both variables (Fig. 1). Full conversion of NIPAM typically occurred within 6 h, while >95% of VAc was consumed after 15 h. As a result of the rapid conversion of NIPAM in the early stages of the reaction, the mole fraction of NIPAM in the feed (f_{NIPAM}) decreased as a function of overall conversion (Fig. 1a). Details related to conversion *vs.* time data of experimental series A and B (Table 1), and additional experiments can be found in Table S1 and Fig. S2–S4 in the ESI.†

Fitting this data to the integrated form of the terminal polymerization model (the Skeist equation[35]) gave best estimates for the reactivity ratios of NIPAM and VAc of 26 (r_{NIPAM}) and 0.062 (r_{VAc}). The 95% joint confidence interval is highly correlated and covers the region $15 < r_{NIPAM} < 42$ and $0 < r_{VAc} < 0.15$ (Fig. 1b).

These reactivity ratios were used to estimate the variation of composition along an average polymer chain as is depicted in

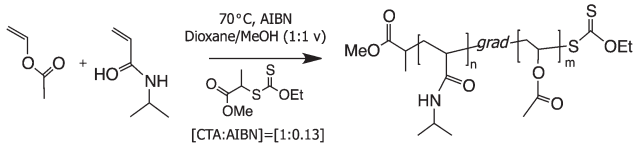

Scheme 2 RAFT copolymerization of NIPAM and VAc in the presence of *O*-ethyl-*S*-1-methoxycarbonylethyl xanthate.

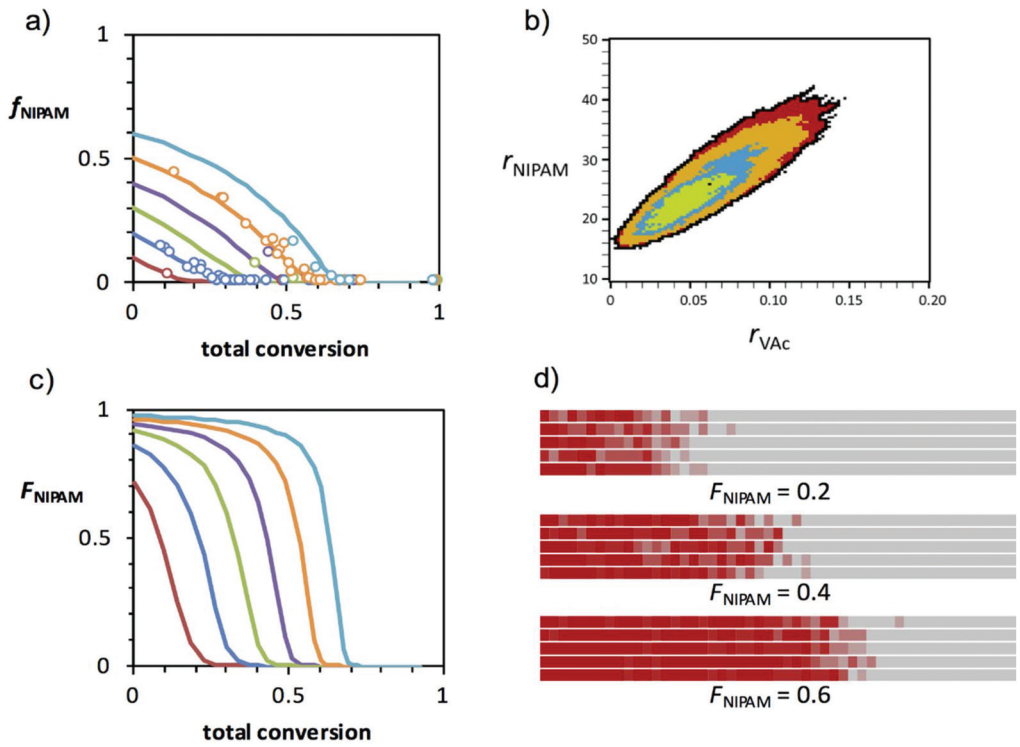

Fig. 1 (a) Mole fraction of NIPAM (f_{NIPAM}) as a function of total monomer conversion in copolymerization of NIPAM and VAc. Lines represent model best fit for initial f_{NIPAM} ranging from 0.1 to 0.6. (b) 95% joint confidence interval for reactivity ratios of NIPAM and VAc. Internal contours represent 50%, 70% and 90% joint confidence intervals. (c) F_{NIPAM} *vs.* conversion for initial f_{NIPAM} ranging from 0.1 to 0.6 (d) simulated chains for NIPAM contents of 20%, 40% and 60%. Five chains of DP = 250 are shown for each composition. Each colored block represents 5 monomer units and is colored according to its NIPAM content (red = 100% NIPAM, gray = 0% NIPAM). Full conversion *vs.* time details can be found in the ESI.†

Fig. 1c. In addition, Fig. 1d shows a schematic representation of the copolymer composition as a function of F_{NIPAM} for five typical polymer chains that contain an equal number of units (DP = 250). For example, the simulated chains for F_{NIPAM} = 0.6 contain initial NIPAM-rich segments with some VAc defects, followed by a smooth transition to a final VAc-rich segment. This visualization emphasizes the discrete structure of the polymer chains and the interchain variation in composition, information which is lost in the global composition *vs*. conversion curve of Fig. 1c. More simulated polymer sequences are displayed in Fig. S5 in the ESI.†

While the number-average molar mass increased monotonically with conversion (Fig. 2), consistent with a reversible deactivation radical polymerization, the molar masses obtained were lower than expected. The discrepancy in molar mass increased as the NIPAM content decreased. This inconsistency may be due to a number of factors, including chain transfer to monomer, solvent, and polymer, which can be pronounced in VAc polymerizations due to the instability of the propagating radical.[17] The use of polystyrene calibration introduces a further source of error to the determination of molar mass.[36] Fig. 3 displays SEC traces of some selected experiments, whereas all SEC traces obtained in this investigation are summarized in Fig. S6 in the ESI.†

In the case of the lower molar mass polymers (Series B in Table 1), the dispersity increased in the final stages of the reaction, most markedly for polymers containing 10–30 mol% of NIPAM. Similar increases in dispersity are frequently observed in the final stages of xanthate-mediated RAFT polymerizations of VAc, and occur as a result of chain transfer to polymer and the gradual accumulation of inactive chains due to head-to-head addition.[37] In both series A and B (Table 1), the dispersities at full conversion ranged from 1.4 to 1.5.

The polymerizations exhibited dispersities of up to 1.8 in the early stages of the reaction, when the polymer formed is principally composed of NIPAM units. This reflects the low chain transfer constant (C_{tr}) of the xanthate RAFT agent in polymerization of acrylamides (C_{tr} = 2.3 in the polymerization of dimethylacrylamide).[38] The molar mass distributions tended to narrow at higher conversions once the NIPAM was consumed, reflecting the much higher C_{tr} of xanthates in the VAc polymerization ($C_{tr} \sim 25$).[37]

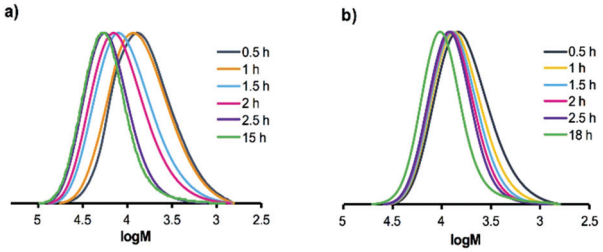

Fig. 3 Representative SEC traces showing the evolution of molar mass with reaction time for monomer : RAFT agent ratios of 250 : 1 (a) and 100 : 1 (b) and NIPAM content of 30 mol%.

Thermal properties

Linear gradient copolymers show unique thermal properties resulting from the smooth change in repulsive interchain interactions due to the gradual change in composition along the chain.[39] Where statistical copolymers typically show a single, relatively sharp glass transition at a temperature that is intermediate between that of the corresponding homopolymers and block copolymers show two distinct glass transitions as a result of microphase separation, while gradient copolymers show a single, broad glass transition that reflects the broad range of compositions present in the sample.[40–42] As materials absorb energy most efficiently at their T_g, the broad glass transitions of gradient copolymers suggest applications

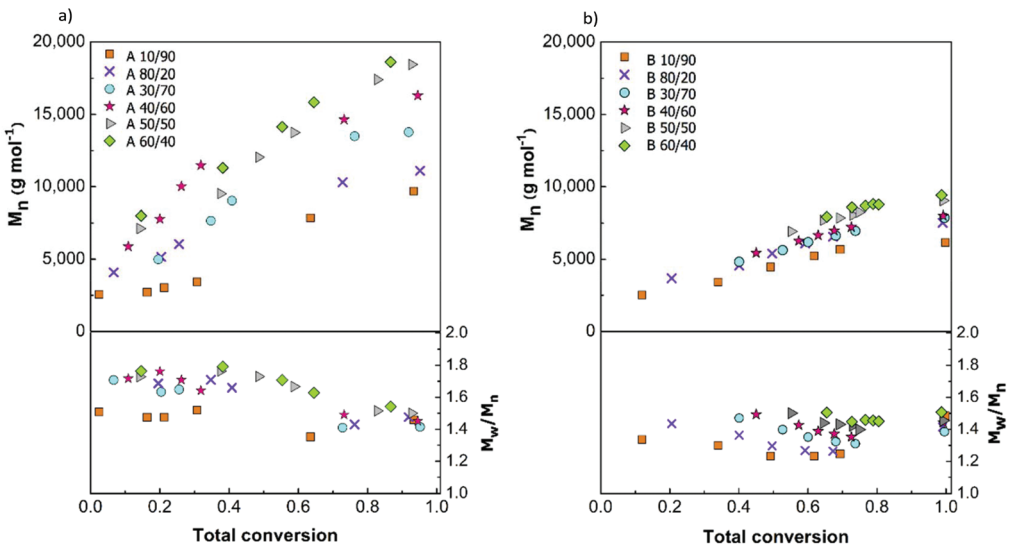

Fig. 2 Number average molar mass (M_n) and dispersity (M_w/M_n) data for polymers produced using monomer to RAFT agent ratios of 250 : 1 (a) and 100 : 1 (b) and NIPAM contents ranging from 10 to 60 mol%.

in shock- and noise-absorbing materials that operate over a wide temperature range.

The copolymers prepared in this study have block-like structures and their composition profiles are highly non-linear. However, they typically show a single, broad glass transition temperature intermediate between that of PVAc (37 °C)[43] and PNIPAM (135 °C),[44] characteristic of a gradient copolymer. Fig. 4 shows first derivatives of DSC heating curves—peaks correspond to the observed glass transitions in the investigated gradient copolymers. The broadest glass transitions were obtained for polymers containing 20–40 mol% of NIPAM. In contrast, a series of block copolymers ($\mathbf{A'}_{20/80}$, $\mathbf{A'}_{30/70}$ and $\mathbf{A'}_{40/60}$) of similar overall composition and molar mass gave two distinct glass transitions for NIPAM contents of 20–40 mol%. Full characterization data for these block copolymers are presented in the ESI.†

As the concentration of PNIPAM ($T_g \approx 130$ °C) increases in the copolymer, the transition shifts toward higher temperatures. These results indicate that even a short transitional segment can impart gradient-like thermal properties to a spontaneous gradient copolymer with a block-like composition profile. Only in the case of sample $\mathbf{A}_{60/40}$, the highest molar mass copolymer with the sharpest transition between NIPAM-rich and VAc-rich segments (Fig. 1c and d), two transitions were observed around 40 °C and 120 °C. This may be attributed to the formation of a *quasi*-block copolymer where both segments are not compatible and the repulsive interactions are confined to the junction of the blocks.

Self-assembly of P(NIPAM-*grad*-VAc) in aqueous solutions

Due to the thermoresponsive properties of PNIPAM,[45] amphiphilic P(NIPAM-*grad*-VAc) copolymers should self-assemble into ordered structures, showing a temperature-dependence on their size near the LCST of PNIPAM (*ca.* 32 °C). Polymers were directly dissolved in water at a concentration of 10 mg mL^{-1}, and the resulting solutions were analyzed by DLS at 25 and 40 °C to reveal the size distribution of self-assembled species (Table 2). In all cases, samples containing only 10% NIPAM were insoluble. Turbid solutions were formed on heating to 40 °C, containing particles of average size ranging from 300 to 600 nm or larger.

At 25 °C, the high molar mass polymers (A series) containing 20–40 mol% NIPAM formed well-defined aggregates of around 30 nm in diameter. Polymers with higher NIPAM content formed solutions containing a broad size distribution of aggregates, possibly due to contamination with PVAc homopolymer. The lower molar mass series of polymers (B series), by contrast, formed relatively large aggregates at 25 °C, ranging from 140 to 230 nm in diameter, while the samples containing 10% and 20% NIPAM were insoluble. Further cooling of these solutions to 5 °C gave smaller aggregates (from 20 to 40 nm) in the case of samples containing 20–40 mol% NIPAM. However these aggregates were less defined than those obtained from the higher-molar mass copolymers, displaying multimodal size distributions (Fig. S8 in the ESI†). This may be related to the greater inter-chain variation in composition obtained using shorter copolymers.

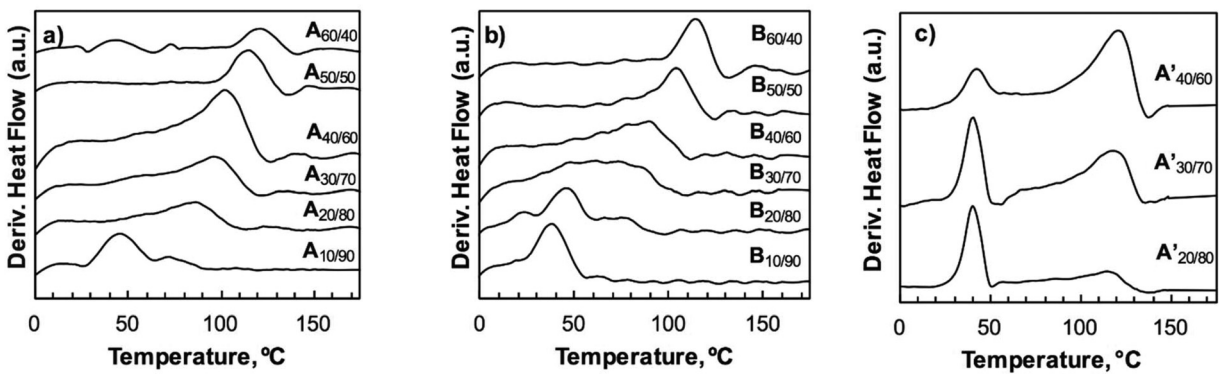

Fig. 4 Derivatives of DSC heating curves series A (a), series B (b) and block copolymers A′ (c).

Table 2 Initial screening of series A and B copolymers. Entries show intensity-average hydrodynamic diameter (nm). Polydispersity is given in parentheses. Figures in italics indicate that the autocorrelation data were poorly fitted by the cumulant method and are indicative only

Sample	T = 25 °C	T = 40 °C	Sample	T = 5 °C	T = 25 °C	T = 40 °C
$A_{10/90}$	Insoluble	Insoluble	$B_{10/90}$	Insoluble	Insoluble	Insoluble
$A_{20/80}$	32 (0.15)	310 (0.08)	$B_{20/80}$	42 (0.21)	Insoluble	Insoluble
$A_{30/70}$	32 (0.10)	*630 (0.5)*	$B_{30/70}$	23 (0.18)	160 (0.20)	350 (0.03)
$A_{40/60}$	27 (0.18)	350 (0.06)	$B_{40/60}$	21 (0.23)	140 (0.23)	*460 (0.4)*
$A_{50/50}$	*28 (0.6)*	550 (0.19)	$B_{50/50}$	*29 (0.7)*	226 (0.33)	*460 (0.3)*
$A_{60/40}$	*24 (0.5)*	*530 (0.5)*	$B_{60/40}$	*300 (0.6)*	*220 (0.5)*	*600 (0.8)*

As the higher molar mass copolymers containing 20–40 mol% NIPAM ($\mathbf{A}_{20/80}$, $\mathbf{A}_{30/70}$ and $\mathbf{A}_{40/60}$) gave well defined aggregates at room temperature and showed a clear thermal response upon heating, these copolymers were studied in more detail, and compared to block copolymers of similar size and composition synthesized by sequential polymerizations ($\mathbf{A'}_{20/80}$, $\mathbf{A'}_{30/70}$ and $\mathbf{A'}_{40/60}$). The size distributions of the aggregates formed at 10 mg mL^{-1} were evaluated by DLS in the range from 25 to 35 °C (Fig. 5). The spontaneous gradient copolymers showed broadly similar behavior to the corresponding block copolymers—small (<100 nm) aggregates were formed at low temperatures, which coalesced into larger particles as the temperature increased. At low temperatures, the size of the block copolymer aggregates increased with the length of the PVAc segment. The gradient copolymers formed smaller aggregates than the corresponding block copolymers and the NIPAM : VAc ratio had no effect on the size of the aggregates. Cryo-TEM analysis revealed that the gradient copolymers formed spherical micellar structures (Fig. 6). For both gradient and block copolymers, the transition between small and large aggregates occurred gradually, with aggregates of intermediate size observed near 30 °C.

The gradual transition was particularly pronounced for the gradient copolymer $\mathbf{A}_{20/80}$, which showed a smooth change in aggregate diameter across the temperature range investigated.

Fig. 7 summarizes the DLS data for block and gradient copolymers, showing the evolution of average size and polydispersity with temperature. It can be observed that where the block copolymers are constant in diameter up to 29 °C, the onset of growth for the gradient copolymers varies for different NIPAM : VAc ratios. This variation was particularly evident in the NMR spectra (Fig. S9–S14 in the ESI†) of 10 mg mL^{-1} solutions of the polymers in D_2O. While the signal intensity of the block copolymers decreased gradually and virtually independently of the NIPAM : VAc ratio in the range from 25 to 35 °C, the signal intensity of gradient copolymers displayed sigmoidal curves with a transition temperature that depended on the VAc content of the copolymer (Fig. 7c and f). The sensitivity of the gradient copolymer cloud points (T_{cp}) to the overall VAc content is likely due to the presence of VAc units in the NIPAM-rich segments. Polymers prepared in the presence of higher levels of VAc contain more VAc in the NIPAM-rich segment (Fig. 1). Previous studies have demonstrated that copolymerization of an LCST monomer with a hydrophobic comonomer reduces the number of hydrogen-bonding interactions between water molecules and the copolymer which decreases the cloud point of the copolymer.[46,47] While for the gradient copolymers, changes in the polymer solubility as revealed by NMR were correlated with changes in aggregate size as revealed by DLS, this was not the case for the block

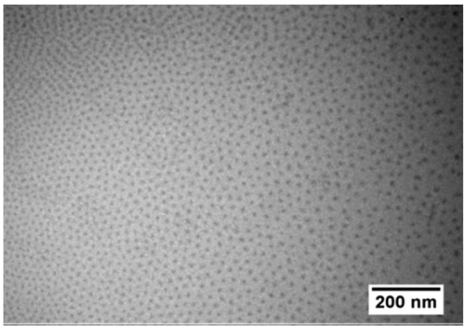

Fig. 6 Cryo-transmission electron micrograph of aggregates of $A_{30/70}$.

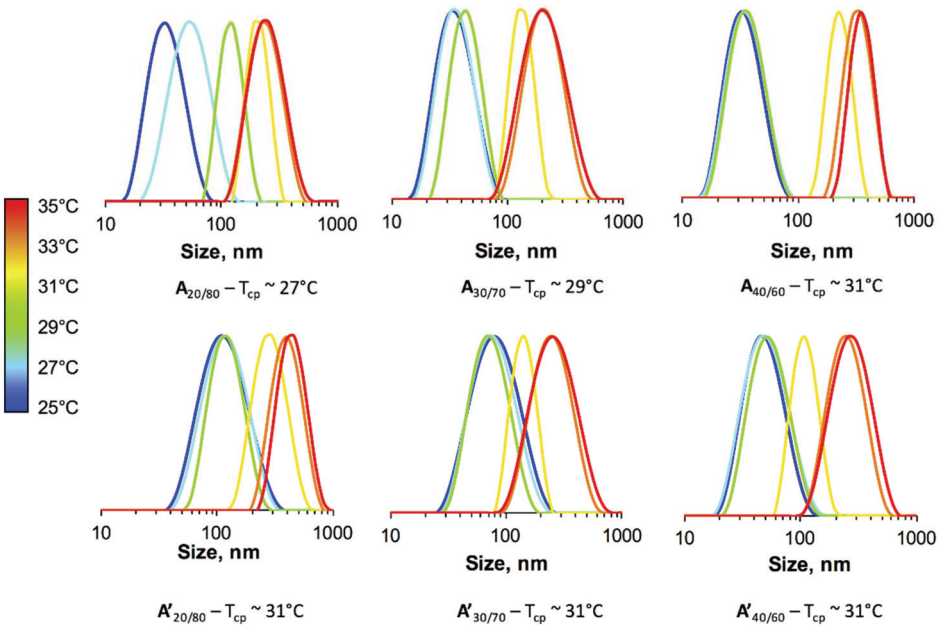

Fig. 5 Hydrodynamic size distributions of 10 mg mL^{-1} aqueous solutions of gradient copolymers $A_{20/80}$ to $A_{40/60}$ and block copolymers $A'_{20/80}$ to $A'_{40/60}$.

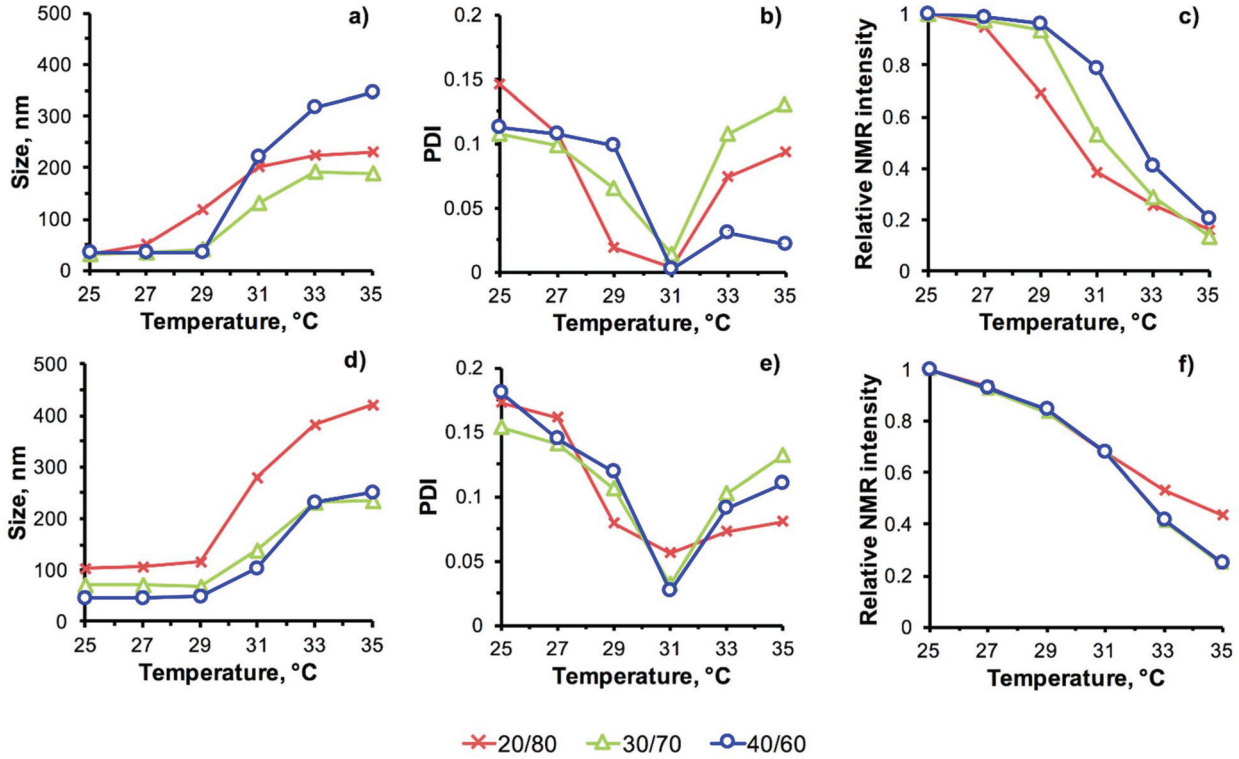

Fig. 7 Hydrodynamic size distributions as obtained by DLS and solubility studies followed by ^{1}H NMR (D_2O) of 10 mg mL^{-1} aqueous solutions of gradient copolymers from $A_{20/80}$ to $A_{40/60}$ (a–c) and block copolymers from $A'_{20/80}$ to $A'_{40/60}$ (d–f) in the temperature range from 25 to 35 °C.

copolymers. We were surprised to observe a gradual decrease in solubility for all block copolymers in the range from 25 to 29 °C, which was not accompanied by a change in hydrodynamic diameter. It has previously been observed that the presence of a hydrophobic end-group shifts the cloud point of PNIPAM to lower temperatures.[48] In this case, the presence of the PVAc block may reduce the cloud point of neighboring PNIPAM segments, so that water is gradually expelled from the aggregate until it becomes unstable at around 31 °C and begins to coalesce with other particles. This process is not accompanied by a change in diameter as the block copolymer aggregates are kinetically frozen.[49] The greater mobility of polymer chains within gradient copolymer aggregates[50–52] allows temperature-induced changes in solubility to be accompanied by rearrangement of the aggregates, resulting in a better correlation between the observed NMR and DLS results.

Conclusions

The xanthate-mediated spontaneous gradient copolymerization of NIPAM and VAc leads to the formation of thermoresponsive amphiphilic copolymers. These copolymers display temperature-dependent changes in aggregation behavior that are similar to those of the corresponding block copolymers, but are prepared in a single step. Despite their block-like composition profiles, the spontaneous gradient copolymers display a single, broad glass transition temperature that is typically observed in linear gradient copolymers. As spontaneous gradient copolymers are significantly easier to prepare than linear forced gradient copolymers, which require a semi-continuous synthesis with careful control over monomer feed, this result should facilitate the preparation of materials with broad glass transitions for shock- and noise-absorbing applications.

The details of their self-assembly behavior in water suggest the formation of dynamic aggregates which respond rapidly to changes in solubility as revealed by NMR analysis, in contrast to the kinetically frozen aggregates formed by block copolymers. The synthetic techniques presented here could readily be transferred to other copolymerization systems, making use of the great variety of commercially-available acrylamide and vinyl ester monomers. As such, spontaneous gradient copolymers have the potential to provide low-cost, accessible alternatives to conventional block copolymers.

Acknowledgements

This research was financially supported by the ASYMCOPO Project, an international collaborative research project of the Deutsche Forschungsgemeinschaft (DFG, Germany) and the Agence Nationale de la Recherche (ANR, France); DFG project: GU 1685/1-1 and ANR project ANR-15-CE08-0039. RYM acknowledges the financial support from CONACyT (Consejo Nacional de Ciencia y Tecnología, México) and the Centro de

Investigación en Química Aplicada (México) to pursue his Ph.D. RYM and CGS also thank CONACyT and DAAD (Deutscher Akademischer Austauschdienst, Germany) for financial support within the framework of the funding program for international mobility PROALMEX 2015 (CONACyT project: 267752 and DAAD project: 57271725). The authors also thank Dr Grit Festag for her valuable support during SEC measurements and the staff of the NMR platform facility at the Faculty of Chemistry and Earth Sciences of the Friedrich Schiller University Jena (http://www.nmr.uni-jena.de/mitarbeiter.php) and Dr Caroline Toppan of the Institut de Chimie de Toulouse (ict.ups-tlse.fr/spectro_rmn.html) for their support during NMR measurements. TEM investigations were performed in the Electron Microscopy facilities of the Jena Center for Soft Matter, which was established by grants of the DFG and the European Regional Development Fund (ERDF).

References

1 D. Roy, W. L. A. Brooks and B. S. Sumerlin, *Chem. Soc. Rev.*, 2013, **42**, 7214–7243.
2 T. Kawaguchi, Y. Kojima, M. Osa and T. Yoshizaki, *Polym. J.*, 2008, **40**, 455–459.
3 S. Hocine and M.-H. Li, *Soft Matter*, 2013, **9**, 5839–5861.
4 M. A. Ward and T. K. Georgiou, *Polymers*, 2011, **3**, 1215.
5 A. P. Vogt and B. S. Sumerlin, *Soft Matter*, 2009, **5**, 2347–2351.
6 L. Despax, J. Fitremann, M. Destarac and S. Harrisson, *Polym. Chem.*, 2016, **7**, 3375–3377.
7 D. J. Keddie, *Chem. Soc. Rev.*, 2014, **43**, 496–505.
8 U. Beginn, *Colloid Polym. Sci.*, 2008, **286**, 1465–1474.
9 F. Ercole, N. Malic, S. Harrisson, T. P. Davis and R. A. Evans, *Macromolecules*, 2010, **43**, 249–261.
10 K. J. Sykes, S. Harrisson and D. J. Keddie, *Macromol. Chem. Phys.*, 2016, **217**, 2310–2320.
11 C. Guerrero-Sanchez, S. Harrisson and D. J. Keddie, *Macromol. Symp.*, 2013, **325–326**, 38–46.
12 S. Harrisson, F. Ercole and B. W. Muir, *Polym. Chem.*, 2010, **1**, 326–332.
13 S. Harrisson and K. L. Wooley, *Chem. Commun.*, 2005, 3259–3261.
14 W. S. Ng, E. Forbes, G. V. Franks and L. A. Connal, *Langmuir*, 2016, **32**, 7443–7451.
15 U. Khan, P. May, H. Porwal, K. Nawaz and J. N. Coleman, *ACS Appl. Mater. Interfaces*, 2013, **5**, 1423–1428.
16 J. Varshosaz, M. Jannesari, M. Morshed and M. Zamani, *Int. J. Nanomed.*, 2011, **6**, 993.
17 S. Harrisson, X. Liu, J.-N. Ollagnier, O. Coutelier, J.-D. Marty and M. Destarac, *Polymers*, 2014, **6**, 1437.
18 E. Read, A. Guinaudeau, D. James Wilson, A. Cadix, F. Violleau and M. Destarac, *Polym. Chem.*, 2014, **5**, 2202–2207.
19 D. Matioszek, P.-E. Dufils, J. Vinas and M. Destarac, *Macromol. Rapid Commun.*, 2015, **36**, 1354–1361.
20 P. Chapon, C. Mignaud, G. Lizarraga and M. Destarac, *Macromol. Rapid Commun.*, 2003, **24**, 87–91.
21 D. Taton, A.-Z. Wilczewska and M. Destarac, *Macromol. Rapid Commun.*, 2001, **22**, 1497–1503.
22 S. Sistach, M. Beija, V. Rahal, A. Brûlet, J.-D. Marty, M. Destarac and C. Mingotaud, *Chem. Mater.*, 2010, **22**, 3712–3724.
23 D. J. Keddie, C. Guerrero-Sanchez, G. Moad, E. Rizzardo and S. H. Thang, *Macromolecules*, 2011, **44**, 6738–6745.
24 R. Nicolay, Y. Kwak and K. Matyjaszewski, *Chem. Commun.*, 2008, 5336–5338.
25 J. J. Haven, C. Guerrero-Sanchez, D. J. Keddie and G. Moad, *Macromol. Rapid Commun.*, 2014, **35**, 492–497.
26 J. J. Haven, C. Guerrero-Sanchez, D. J. Keddie, G. Moad, S. H. Thang and U. S. Schubert, *Polym. Chem.*, 2014, **5**, 5236–5246.
27 C. Guerrero-Sanchez, D. J. Keddie, S. Saubern and J. Chiefari, *ACS Comb. Sci.*, 2012, **14**, 389–394.
28 X. Liu, O. Coutelier, S. Harrisson, T. Tassaing, J.-D. Marty and M. Destarac, *ACS Macro Lett.*, 2015, **4**, 89–93.
29 M. Van Den Brink, A. M. Van Herk and A. L. German, *J. Polym. Sci., Part A: Polym. Chem.*, 1999, **37**, 3793–3803.
30 G. Moad, E. Rizzardo and S. H. Thang, *Chem. – Asian J.*, 2013, **8**, 1634–1644.
31 A. Favier and M.-T. Charreyre, *Macromol. Rapid Commun.*, 2006, **27**, 653–692.
32 Y. K. Chong, J. Krstina, T. P. T. Le, G. Moad, A. Postma, E. Rizzardo and S. H. Thang, *Macromolecules*, 2003, **36**, 2256–2272.
33 M. Destarac, D. Charmot, X. Franck and S. Z. Zard, *Macromol. Rapid Commun.*, 2000, **21**, 1035–1039.
34 M. Destarac, A. Papon, E. Van Gramberen and K. Karagianni, *Aust. J. Chem.*, 2009, **62**, 1488–1491.
35 I. Skeist, *J. Am. Chem. Soc.*, 1946, **68**, 1781–1784.
36 T. Gruendling, T. Junkers, M. Guilhaus and C. Barner-Kowollik, *Macromol. Chem. Phys.*, 2010, **211**, 520–528.
37 P. E. Dufils, G. David, B. Boutevin, G. Woodward, G. Otter, A. Guinaudeau, S. Mazières and M. Destarac, *J. Polym. Sci., Part A: Polym. Chem.*, 2012, **50**, 1997–2007.
38 E. Girard, T. Tassaing, J.-D. Marty and M. Destarac, *Polym. Chem.*, 2011, **2**, 2222–2230.
39 A. I. Buzin, M. Pyda, P. Costanzo, K. Matyjaszewski and B. Wunderlich, *Polymer*, 2002, **43**, 5563–5569.
40 J. Kim, M. M. Mok, R. W. Sandoval, D. J. Woo and J. M. Torkelson, *Macromolecules*, 2006, **39**, 6152–6160.
41 J. Zhang, J. Li, L. Huang and Z. Liu, *Polym. Chem.*, 2013, **4**, 4639–4647.
42 S. Jouenne, J. A. González-León, A.-V. Ruzette, P. Lodefier, S. Tencé-Girault and L. Leibler, *Macromolecules*, 2007, **40**, 2432–2442.
43 T. Sato and T. Okaya, *Polym. J.*, 1992, **24**, 849–856.
44 R. G. Sousa, W. F. Magalhães and R. F. S. Freitas, *Polym. Degrad. Stab.*, 1998, **61**, 275–281.
45 C. M. Z. Cristiano, V. Soldi, C. Li, S. P. Armes, C. Rochas, I. Pignot-Paintrand and R. Borsali, *Macromol. Chem. Phys.*, 2009, **210**, 1726–1733.

46 L. Etchenausia, A. M. Rodrigues, S. Harrisson, E. Deniau Lejeune and M. Save, *Macromolecules*, 2016, **49**, 6799–6809.
47 D. Fournier, R. Hoogenboom, H. M. L. Thijs, R. M. Paulus and U. S. Schubert, *Macromolecules*, 2007, **40**, 915–920.
48 Y. Xia, N. A. D. Burke and H. D. H. Stöver, *Macromolecules*, 2006, **39**, 2275–2283.
49 T. Nicolai, O. Colombani and C. Chassenieux, *Soft Matter*, 2010, **6**, 3111–3118.
50 S. Okabe, K. Seno, S. Kanaoka, S. Aoshima and M. Shibayama, *Macromolecules*, 2006, **39**, 1592–1597.
51 R. W. Sandoval, D. E. Williams, J. Kim, C. B. Roth and J. M. Torkelson, *J. Polym. Sci., Part B: Polym. Phys.*, 2008, **46**, 2672–2682.
52 H. M. L. Lambermont-Thijs, M. J. H. C. Jochems, R. Hoogenboom and U. S. Schubert, *J. Polym. Sci., Part A: Polym. Chem.*, 2009, **47**, 6433–6440.